

Electromagnetic Properties Monitoring to Detect Different Biodegradation Kinetics in Hydrocarbon-Contaminated Soil

Original

Electromagnetic Properties Monitoring to Detect Different Biodegradation Kinetics in Hydrocarbon-Contaminated Soil / Vergnano, A., Raffa, C.M., Godio, A., Chiampo, F.. - In: SOIL SYSTEMS. - ISSN 2571-8789. - 6:2(2022), p. 48. [10.3390/soilsystems6020048]

Availability:

This version is available at: 11583/2974617 since: 2023-01-14T16:58:21Z

Publisher:

MDPI

Published

DOI:10.3390/soilsystems6020048

Terms of use:

This article is made available under terms and conditions as specified in the corresponding bibliographic description in the repository

Publisher copyright

(Article begins on next page)



Electromagnetic Properties Monitoring to Detect Different Biodegradation Kinetics in Hydrocarbon-Contaminated Soil

Andrea Vergnano ¹, Carla Maria Raffa ², Alberto Godio ¹ and Fulvia Chiampo ^{2,*}

¹ Department of Environment, Land, and Infrastructure Engineering, Politecnico di Torino, Corso Duca degli Abruzzi 24, 10129 Torino, Italy; andrea.vergnano@polito.it (A.V.); alberto.godio@polito.it (A.G.)

² Department of Applied Science and Technology, Politecnico di Torino, Corso Duca degli Abruzzi 24, 10129 Torino, Italy; carla.raffa94@gmail.com

* Correspondence: fulvia.chiampo@polito.it; Tel.: +39-011-090-4685

Abstract: The electromagnetic properties (electrical permittivity and electrical conductivity) of three different soil mesocosms polluted with diesel oil were monitored using a time-domain reflectometry probe for 8 months. The main target of the research was to establish a relationship between the development of biological activity within the mesocosms and the temporal behaviour of electromagnetic properties. The trend of the electromagnetic properties exhibited different responses that could be related to the composition of the mesocosms and their variation with time during the runs. We considered three different mesocosms with similar soil conditions and the same diesel oil concentration: porosity of 45%, volumetric diesel oil content of 9%, and volumetric water content of 15%. The first one was subjected to a natural attenuation (NA), the second one was biostimulated without inoculation (BS), and the third one was biostimulated with inoculation (BS + IN). The biostimulated mesocosms showed a marked decrease in electrical permittivity and electrical conductivity, whereas the naturally attenuated mesocosm did not show these variations. Between the biostimulated mesocosms, the inoculated one showed the fastest variations in the electromagnetic properties. The microbial activity and the pollutant degradation were evidenced by the analyses performed at the end of the experiment. As demonstrated by the results for the fluorescein diacetate analysis, the microbial activity was a bit higher for the inoculated microcosm, which also showed faster variations of the electromagnetic properties. In the biostimulated mesocosms, the removal of diesel oil was 66% and 72%, respectively. With natural attenuation, there was a limited removal efficiency, in the order of 2%. Even if the electromagnetic properties evidenced different kinetics of bioremediation in BS and BS + IN, both were able to successfully degrade similar percentages of the contaminant after 8 months. The long monitoring revealed that a substantial decrease in the electromagnetic properties happened only in the first month after contamination. Additionally, an increasing trend of the permittivity was detected in the following months, before reaching a steady-state condition. This study revealed that biodegradation processes with acceptable overall removal efficiency can be monitored successfully by observing the variations in the electromagnetic properties.

Keywords: diesel oil; aerobic soil remediation; time-domain reflectometry; electrical permittivity; electrical conductivity



Citation: Vergnano, A.; Raffa, C.M.; Godio, A.; Chiampo, F. Electromagnetic Properties Monitoring to Detect Different Biodegradation Kinetics in Hydrocarbon-Contaminated Soil. *Soil Syst.* **2022**, *6*, 48. <https://doi.org/10.3390/soilsystems6020048>

Academic Editor: Richard Wilkin

Received: 4 April 2022

Accepted: 19 May 2022

Published: 24 May 2022

Publisher's Note: MDPI stays neutral with regard to jurisdictional claims in published maps and institutional affiliations.



Copyright: © 2022 by the authors. Licensee MDPI, Basel, Switzerland. This article is an open access article distributed under the terms and conditions of the Creative Commons Attribution (CC BY) license (<https://creativecommons.org/licenses/by/4.0/>).

1. Introduction

The remediation of soils contaminated with hydrocarbons is an old challenge, and several techniques and approaches were tested. Notwithstanding this, it is not won, yet and the research can still improve and enhance the current knowledge. The question involves expertise from different sectors, and their cooperation is a way to better clarify the features of the involved processes and their monitoring.

Among the techniques, bioremediation is one option, due to its low cost and application easiness, especially when aerobic remediation is adopted [1]. However, with this

technique, many issues must be faced and solved. First, the optimal operative conditions must be known to get the best results in terms of overall pollution removal [2]. These parameters are usually optimized by experimental runs carried out in the laboratory and then in situ. These are preliminary and compulsory activities. Given the exploitation of biological processes to remove pollution, the parameters are related to microbial metabolism, and the main ones are the water content and the ratio of carbon to nitrogen (C/N) [3].

Very often, little attention is given to the monitoring of the process, notwithstanding its relevance for the remediation success. Monitoring should be considered as an action supporting the whole process, and as for the technique itself, its easiness and cost are characteristics to be assessed.

The integration of geochemical, biological, and geophysical methods as a tool for monitoring hydrocarbon contaminated sites is often required for assessing the natural attenuation processes taking place in soil and groundwater [4]. A recent analysis of the natural attenuation of hydrocarbons as remediation action in a contaminated site using a combination of several investigation methods (bio-molecular analysis, isotope analysis) was discussed by Zanini et al. [5]. All the studies on the effectiveness and reliability of the monitoring approach require specific calibration and validation starting from laboratory-scale experiments. Particularly, when geophysical methods are involved in a preliminary screening of the contaminated site, the specific response of the soil system to the different factors affecting the geophysical parameters must be evaluated carefully at the laboratory scale [6]. The most sensitive parameters are the electrical conductivity and permittivity, due to their sensitivity to the fluid content and kind in the soil pore volume, and because the long-term monitoring of those parameters could be easily performed both in the laboratory and at the field scale [7,8]. The main advantages of monitoring these properties with geophysical methods are reported in the literature [4,9–11] and the limited perturbation introduced by the probe itself, the possibility to relate the observed parameters to the physical and chemical behaviour of the mesocosm, and the easiness to use of this system to monitor a run for a long time.

Previous literature dealt with the time-lapse monitoring of electromagnetic properties to detect biodegradation processes of contaminants at the lab scale. Mori et al. [12] set up microcosms with continuous nutrient fluid addition, measuring the electrical conductivity of the outflow. Masy et al. [13] studied the variation of the electrical resistivity (reciprocal of electrical conductivity) with an experiment that simulated an electrical resistivity tomography, a common geophysical method applied at a field scale. These experiments evidenced fluctuations in the properties monitored but required complex designs.

To decrease the complexity of previous experimental setups, we chose to simulate the bioremediation of contaminated soil through a simple setup, based on the experience of previous work. In Raffa et al. [14], the operative conditions were optimized at the laboratory scale (microcosms). Regarding the monitoring, Vergnano et al. showed that electromagnetic properties variations can be detected with good performance with lab-scale geophysical instruments in a system where bioremediation is occurring [15,16]. We set up three mesocosms, to say plexiglass columns containing soil, water, and diesel oil such that unsaturated conditions could favour the aeration of the soil matrix. In the first mesocosm, we monitored the natural attenuation, that is the removal of contaminant without artificial treatment. The other two mesocosms were biostimulated by adding a nutrient solution suitable to enhance bacterial growth. One of the two was also inoculated with a small portion of soil containing microorganisms acclimated to diesel oil biodegradation. We monitored the bio-geochemical behaviour of the mesocosms by time-lapse measuring the electrical resistivity and electrical permittivity. The measurements were based on the adoption of the time-domain reflectometer approach. With this system, the probe can observe simultaneously both the electrical resistivity and the electrical permittivity of the materials under contact. At the end of the experiment, we collected soil samples to analyse the residual diesel oil concentration after bioremediation, and to evaluate the microbial activity through a fluorescein diacetate (FDA) method. Comparing geophysical and bio-

geochemical methods, we checked if the trend of the measured electromagnetic properties exhibited a response that could be related to the specific mixture of the mesocosm and its variation with time during the experiment.

The main novelty of our work regards the investigation of how geophysical signatures of soil are sensitive to the operative conditions of the biodegradation processes. The proposed method is rather simple to build and run compared to others discussed in previous literature, as it does not require flux recirculation, and TDR probes are not expensive nor difficult to use. This may be seen as a great advantage in the frame of field applications where several operative conditions must be tested before a field implementation of bioremediation techniques.

2. Materials and Methods

2.1. Experimental Set-Up

The experiment was carried out in three Plexiglas columns, with a diameter equal to 19 cm. Each column was filled with 17 cm (NA) and 20 cm (BS, BS + IN) of soil, sieved to obtain a particle size distribution between 0.15 and 2 mm, and artificially polluted with diesel oil. The soil mass was equal to 7.3 kg (NA), and 8.4 kg (BS, BS + IN).

The first mesocosm was hydrated with tap water to simulate natural attenuation (NA). The others were hydrated by adding a nutrient solution suitable to biostimulate the bacterial growth and reach the optimal value of carbon to nitrogen ratio (C/N), as by the results of a previous study [14]. One of them was studied without any other change of its characteristics (BS), while the other was also inoculated with soil rich in indigenous hydrocarbon-degrading microorganisms (BS + IN) deriving from previous runs done at a smaller scale, on the same type of soil and with the same contaminant. The concentration of microorganisms in the inoculum, as colony-forming units (CFU) per gram of soil, is reported in Table 1.

Table 1. Main parameters of the mesocosms.

Parameter/Mesocosm	Natural Attenuation (NA)	Biostimulation (BS)	Biostimulation + Inoculum (BS + IN)
Soil mass (kg)	7.3	8.4	8.4
Diameter of soil column (cm)	19	19	19
Height of soil (cm)	17	20	20
Soil volume (dm ³)	4.9	5.7	5.7
Real density of soil (kg·dm ⁻³)	2.7	2.7	2.7
Apparent density of soil (kg·dm ⁻³)	1.48	1.48	1.48
Porosity (Volume _{pores} ·Volume _{tot} ⁻¹)	0.45	0.45	0.45
Quantity of inoculum (kg)	-	-	0.65
Inoculum/soil ratio (kg _{inoculum} ·kg _{soil} ⁻¹)	-	-	8%
Initial oil-degrading microorganisms (CFU·g _{soil} ⁻¹)	-	-	6.59 × 10 ⁴
Oil saturation (Volume _{oil} ·Volume _{pores} ⁻¹)	0.20	0.20	0.20
Volumetric oil content (Volume _{oil} ·Volume _{tot} ⁻¹)	0.09	0.09	0.09
Oil content (kg _{oil} ·kg _{soil} ⁻¹)	0.05	0.05	0.05
Water saturation (Volume _{water} ·Volume _{pores} ⁻¹)	0.33	0.33	0.33
Volumetric water content (Volume _{water} ·Volume _{tot} ⁻¹)	0.15	0.15	0.15
Moisture content (kg _{water} ·kg _{soil} ⁻¹)	0.10	0.10	0.10
Carbon to nitrogen ratio (g _C ·g _N ⁻¹)	-	135	135
Electrical conductivity of the nutrient solution (S·m ⁻¹)	0.054	1.45	1.45
Experimental duration (d)	193	228	228

Table 1 reports the characteristics of the studied mesocosms at the starting time of each run.

The test lasted 193 days for the NA mesocosm, and 228 days for the others. For the NA mesocosm, the run was stopped when it was evident that the geophysical parameters did not change, while the monitoring of BS and BS + IN mesocosms was prolonged for

further 35 days. At the end of each test, soil samples were collected according to Standard Sampling [17].

In the centre of each column, a time-domain reflectometry (TDR) probe was located and connected to the digital logger.

Figure 1 shows the experimental setup.

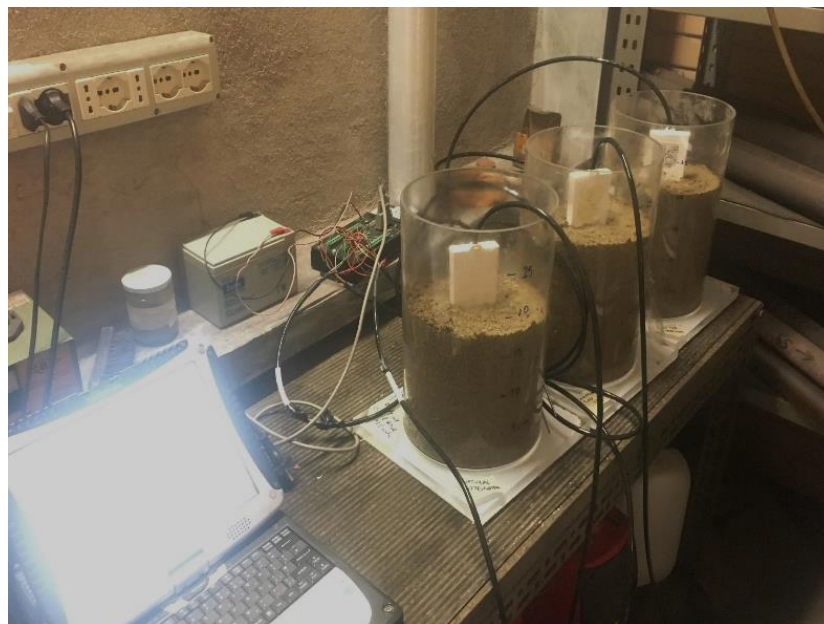


Figure 1. Experimental setup. The three columns are the three mesocosms. A white TDR probe is inserted in each of them and connected to the black datalogger behind.

2.2. Time-Domain Reflectometry (TDR)

Time-domain reflectometry is a method to observe the electromagnetic properties of soil based on the travel time of a high-frequency electromagnetic pulse through the soil itself. The travel time is used to calculate the electrical permittivity of the soil, which controls the velocity of propagation of electromagnetic signals. The TDR probes can be inserted directly into the soil for in situ measurement at the desired soil depth and can be also adopted for monitoring time-lapse behaviour as they can be attached to a data logger for ongoing measurements. The permittivity of the soil is strongly related to the fluid content due to the unique properties of the water molecule. The electrical permittivity of water is about 80 with a dependency on the temperature, while the electrical permittivity of most solid minerals is between 2 and 7 (the air permittivity is equal to 1). Therefore, the soil's electrical permittivity is an indicator of the water content inside the soil itself.

The electrical conductivity is estimated by analysing the attenuation of the amplitude of the signal which propagates along with the probe, being reflected at the end of the probe itself. In soil, the electrical conductivity is affected by the fluid content and salinity. Temperature influences conductivity, too.

In this study, the monitoring of electrical conductivity and electrical permittivity was carried out with Campbell CS655 TDR probes, immersed in the soil for their entire length (12 cm). The spacing between the rods is 32 mm, and their diameter is 3.2 mm. Our probe also measured the electrical conductivity of soil, by measuring the reduction of voltage along the sensor after exciting the rods with a 100 kHz waveform.

Each probe measured temperature, electrical conductivity, and electrical permittivity for 228 days (193 days for NA), storing the recorded data in a datalogger.

2.3. Fluorescein Diacetate (FDA) Analysis

To evaluate microbial activity, the hydrolysis of fluorescein diacetate (FDA) was measured, according to Schnurer and Rosswall method [18], and modified by Adam and Duncan [19].

FDA can be hydrolysed by different enzymes present in the soil, like protease, lipase, and esterase. The product of this reaction is fluorescein, and its concentration can be measured through spectrophotometric analysis (this compound has intense yellow colour).

This method is a simple, fast, and reliable technique to determine overall microbial activity.

The methodology provides two solutions:

- Potassium phosphate buffer: $8.7 \text{ kg}\cdot\text{m}^{-3}$ of K_2HPO_4 and $1.3 \text{ kg}\cdot\text{m}^{-3}$ of KH_2PO_4 at $\text{pH} = 7.6$;
- FDA stock solution in acetone: 0.1 g of FDA and 50 mL of acetone.

From each sample, 2 g of wet soil were taken and mixed with 15 mL of potassium phosphate buffer and 100 μL of FDA stock solution in acetone. The solution was agitated for 1 h at 50 rpm. Then, to stop the hydrolysis reaction, 15 mL of acetone was added. The samples were centrifugated at 6000 rpm for 5 min and then filtered through a 1.2 μm filter to remove possible colloidal particles. Solution absorbance was measured with spectrophotometric analysis at 490 nm and referring to the blank that contained only the potassium phosphate solution.

In each mesocosm, the fluorescein diacetate analysis was carried out in two soil samples at the end of the run:

- Soil sample 1 was taken after mixing the whole soil mass;
- Soil sample 2 was taken from the bottom of the column.

2.4. Diesel Oil Extraction and Gas Chromatograph Analysis

The diesel oil was extracted from each mesocosm applying the EPA method 3546 (moisture 15–30% by mass) [20], based on microwave heating. In this method, 2 g of soil was mixed with 30 mL of solvent (acetone and n-hexane with a ratio of 1:1 by volume) and 2 g of anhydrous sodium sulphate to dry the soil. The sample was heated at 110 °C for 15 min through microwaves, kept at this temperature for 10 min, and then cooled for 20 min. After the extraction, the sample was filtered through a 0.45 μm filter. This procedure was replicated, thus obtaining two extracts.

The diesel oil concentration was quantified using gas chromatography (GC-FID), with the EPA method 8015 [21]. The gas chromatograph was equipped with a flame ionization detector and DB-5 fused silica capillary column, operated with helium as the carrier. The injector and detector were maintained at 220 °C and 250 °C, respectively. The following temperature program was used: initial temperature of 50 °C, ramp to 320 °C at $8 \text{ }^\circ\text{C}\cdot\text{min}^{-1}$, and a constant temperature of 320 °C for 40 min.

The chromatogram was analysed evaluating the peaks between 6 and 33 min since this time range contains the characteristic ones of diesel oil.

The residual diesel oil concentration was calculated using a calibration line achieved with the commercial diesel oil used in the test.

The compounds that characterize the diesel oil were identified by standard kits, namely:

- C7–C30 saturated *n*-alkanes, 1000 $\mu\text{g}\cdot\text{mL}^{-1}$ each component in hexane;
- PAHs (acenaphthylene, anthracene, benzo(α)anthracene, fluorene, phenanthrene, pyrene), 500 $\mu\text{g}\cdot\text{mL}^{-1}$ each component in acetone.

Comparing the retention times of the analysed peaks to the standard ones, the *n*-alkanes from C8 to C24 and six PAHs were determined.

Two gas chromatographic analyses were done for each extract.

2.5. Removal Efficiency

The overall pollutant removal efficiency, Eff%, can be calculated as:

$$\text{Eff\%} = (C_0 - C_1) / C_0 \cdot 100 \quad (1)$$

where C_0 and C_1 are the initial diesel oil concentration and the one at the end of the test, respectively.

2.6. Viscosity

The viscosity is a parameter that depends on the temperature variation and influences the motion of fluids. In the case of contaminated soil, the viscosity of the water-hydrocarbon mixture impacts the propagation of the contaminant plume in the aquifer.

To evaluate the viscosity of the water-diesel oil mixture, the viscosity of each component was assessed.

For a pure compound, this parameter can be evaluated by an empirical equation, containing the influence of the temperature [22]. In conditions of low pressure (1 atm) and $273.16 \text{ K} < T < 646.15 \text{ K}$, the correlation is:

$$\mu = \exp\left(C_1 + \frac{C_2}{T} + C_3 \ln(T) + C_4 T^{C_5}\right) \quad (2)$$

where μ is the viscosity in Pa·s, T is the temperature in K, and C_1, C_2, C_3, C_4, C_5 are experimental coefficients, the value of which depends on the type of liquid. For water, the values of experimental coefficients are $C_1 = -52.843$; $C_2 = 3703.6$; $C_3 = 5.86$; $C_4 = -5.879 \cdot 10^{-29}$; $C_5 = 10$.

Diesel oil viscosity was determined by the well-known relation:

$$\mu = \eta \rho \quad (3)$$

where η is the kinematic viscosity and ρ is the density.

The kinematic viscosity of diesel oil can be determined with the Andrade equation [22]:

$$\eta = eT^3 + fT^2 + gT + h \quad (4)$$

The coefficients $e, f, g,$ and h were determined by Nita et al. [23]: $e = -1 \times 10^{-4} \text{ mm}^2 \cdot (\text{s} \cdot (^\circ\text{C})^3)^{-1}$; $f = 0.0029 \text{ mm}^2 (\text{s} \cdot (^\circ\text{C})^2)^{-1}$; $g = -0.2195 \text{ mm}^2 \cdot (\text{s} \cdot ^\circ\text{C})^{-1}$; and $h = 8.159 \text{ mm}^2 \cdot \text{s}^{-1}$. The temperature must be expressed in $^\circ\text{C}$, and the viscosity η in $\text{mm}^2 \cdot \text{s}^{-1}$.

The density variation with temperature is based on the equation:

$$\rho = AT + B \quad (5)$$

where the experimental parameters are ones defined by Nita et al. [23], namely $A = -0.0007 \text{ g} \cdot (\text{cm}^3 \cdot ^\circ\text{C})^{-1}$ and $B = 0.8939 \text{ g} \cdot \text{cm}^{-3}$, with the temperature in $^\circ\text{C}$, and the density in $\text{g} \cdot \text{cm}^{-3}$.

The viscosity of the immiscible mixture, composed of diesel oil and water is calculated by the equation given by Wen et al. [24], which considers a system composed of water and oil:

$$\mu_m = \mu_o \cdot (1 - \text{WC}) + \mu_w \cdot \text{WC} \quad (6)$$

where μ_o is the diesel oil viscosity, μ_w is the water viscosity, and WC is the volumetric water content, to say the ratio of water volume to total volume ($\text{WC} = V_{\text{water}} \cdot V_{\text{mix}}^{-1}$).

3. Results

3.1. Time-Domain Reflectometry

As aforesaid, the tests lasted until 228 days. During this period, the temperature was not constant, ranging from 30 to 5 $^\circ\text{C}$, and its monitoring is reported in Figure 2.

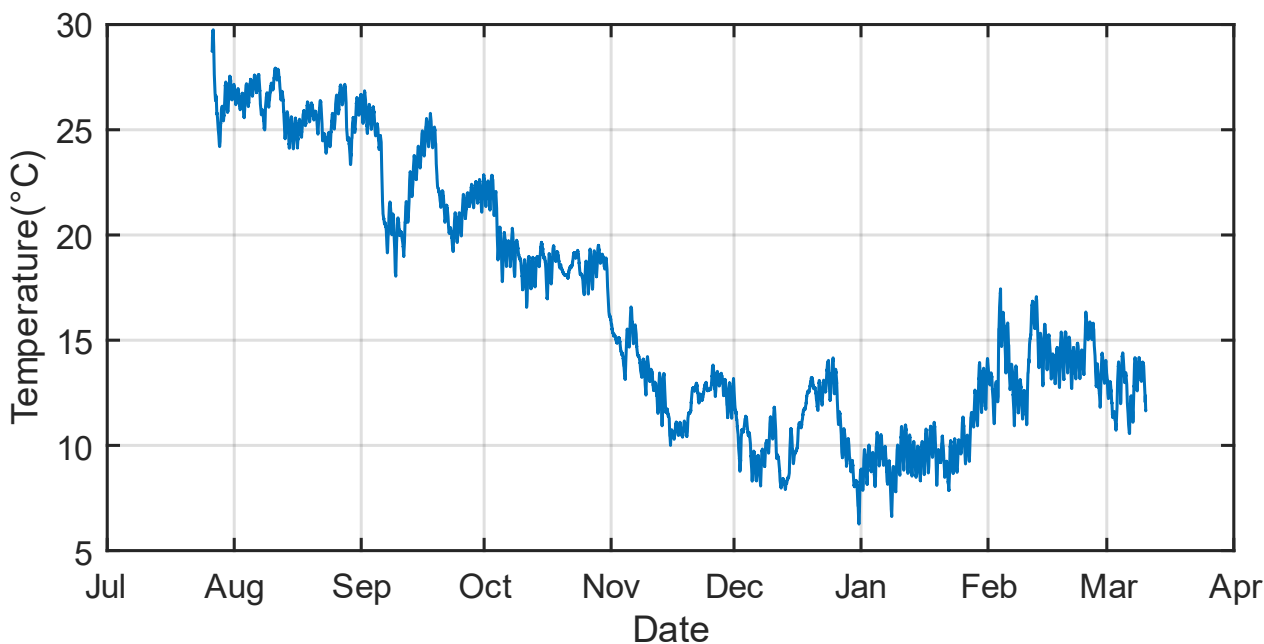


Figure 2. Temperature (°C) of the mesocosms during the test.

The monitoring of the electrical conductivity is shown in Figure 3. As the electrical conductivity is affected by the temperature variation, the trend of the temperature follows a different trend for the electrical conductivity. A gradual decrease in temperature from August up to December is observed. Meanwhile, the electrical conductivity of the biostimulated mesocosms (BS and BS + IN) showed a marked decrease at the very early stage of the experiment (first weeks). This proves the relatively negligible effect of the temperature on the behaviour of electrical conductivity.

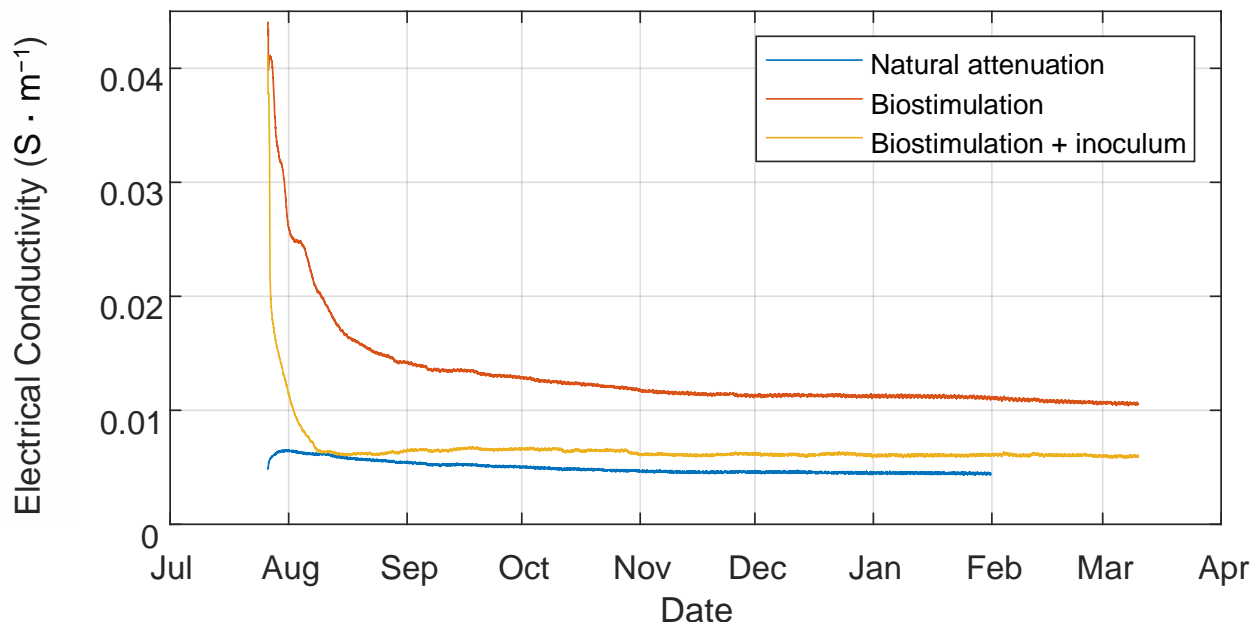


Figure 3. Electrical conductivity of the tested mesocosms corrected for temperature.

The trend of electrical permittivity, which the probe measures separately from the electrical conductivity, pointed out other interesting behaviour (Figure 4).

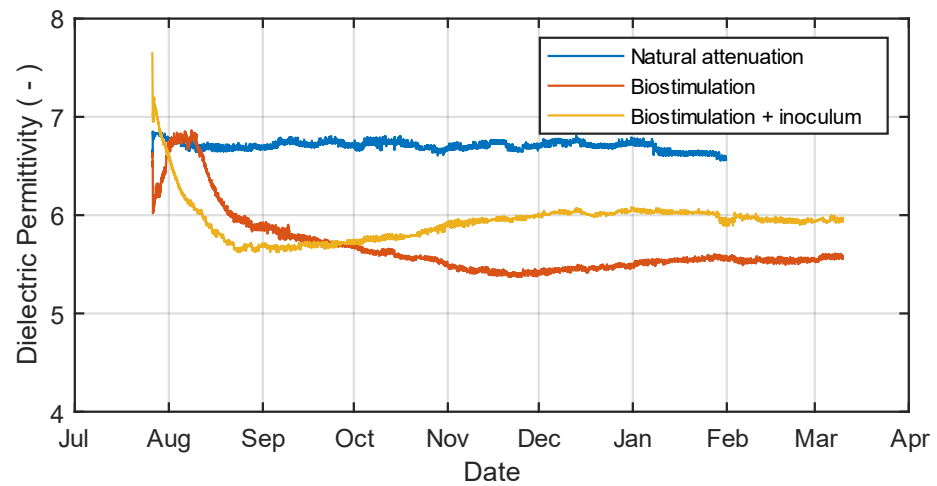


Figure 4. Electrical permittivity of the tested mesocosms.

In Table 2, the asymptotic values of the measured electromagnetic properties are reported.

Table 2. Asymptotic values of the electromagnetic properties measured by TDR probes.

Property	Asymptotic Values		
	Natural Attenuation (NA)	Biostimulation (BS)	Biostimulation + Inoculum (BS + IN)
Electrical conductivity ($S \cdot m^{-1}$)	0.004	0.010	0.006
Electrical permittivity	6.57	5.95	4.43
Volumetric water content ($Volume_{water} \cdot Volume_{tot}^{-1}$)	0.12	0.07	0.10

3.2. Microbial Activity

The fluorescein production was measured at the end of the test to assess the microbial activity in each mesocosm.

Figure 5 reports the results.

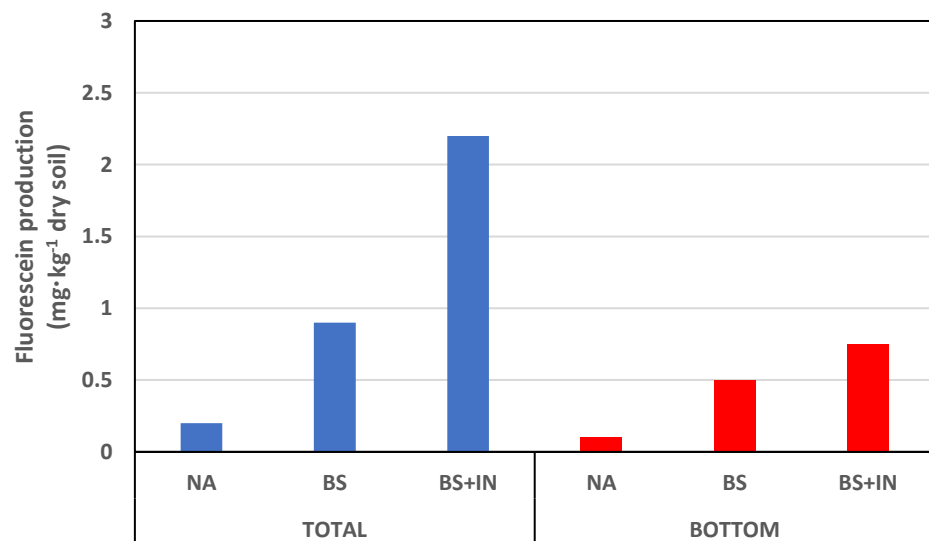
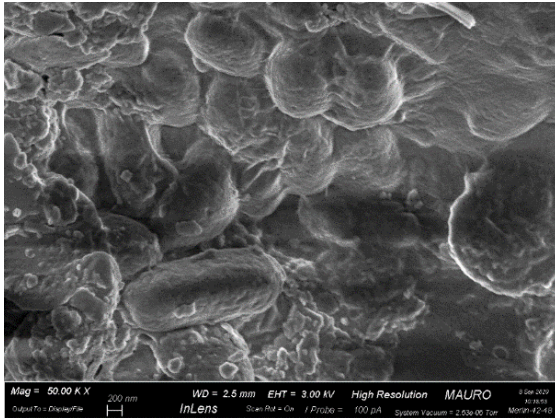


Figure 5. Fluorescein production at $t = 228$ days for BS and BS + IN, and at $t = 193$ days for NA.

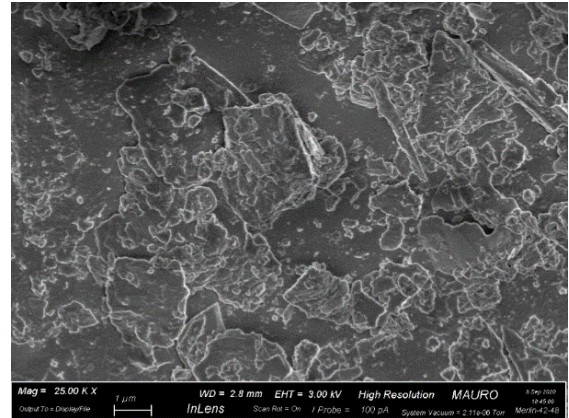
In the BS + IN mesocosm, there is a higher microbial activity than in the others, both in the total sample and in the bottom one.

These results are supported by images taken with the Scanning Electron Microscope at the end of the test, shown in Figure 6, where the BS and BS + IN mesocosms appear populated with many microorganisms.

NA mesocosm

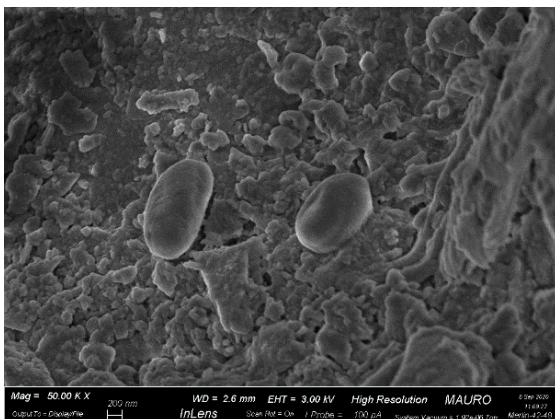


(a)

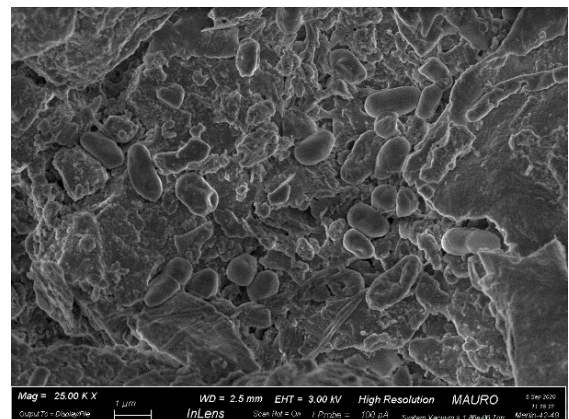


(b)

BS mesocosm

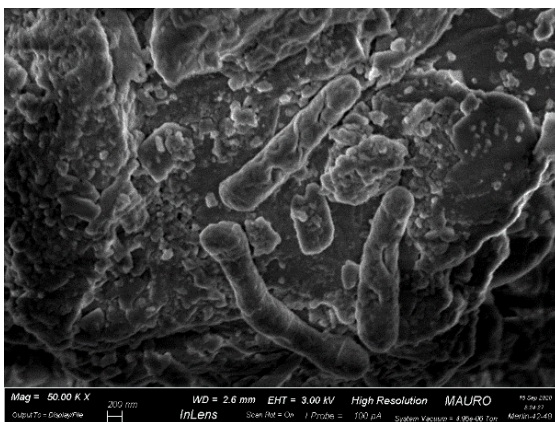


(c)

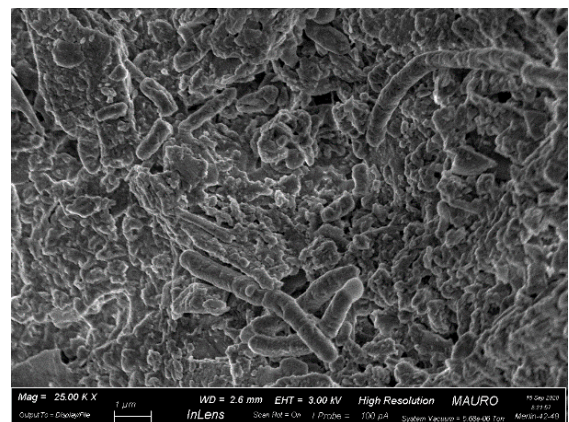


(d)

BS + IN mesocosm



(e)



(f)

Figure 6. SEM images for: (a) central and (b) bottom zone of NA mesocosm; (c,d) superficial zone of BS mesocosm; and (e,f) superficial zone of BS + IN mesocosm.

For the NA microcosm, the presence of microorganisms was evidenced in the centre of the column (Figure 6a); however, on the bottom, no microbial species seem present (Figure 6b).

For the biostimulated microcosms, the images show the presence of a well-developed microbial population. For BS microcosm, the images refer to the superficial zone, while for BS + IN one, they show the system on the column bottom.

3.3. Diesel Oil Removal Efficiency

The quantity of residual diesel oil in the studied mesocosms depends on the operative conditions. As expected, the addition of the mineral solution promoted the biodegradation process. Figure 7 reports the removal efficiency in the tested mesocosms, both in the total system and at the bottom, calculated by Equation (1).

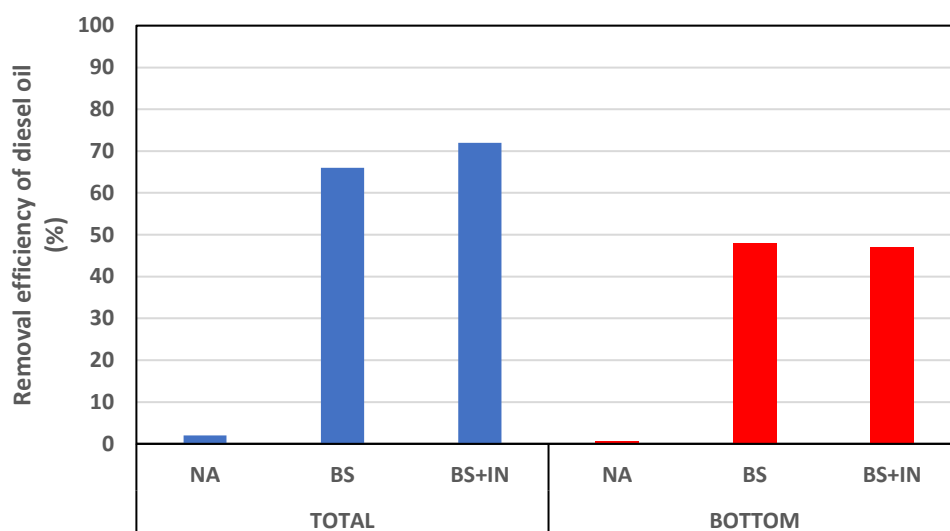


Figure 7. Diesel oil removal efficiency at $t = 228$ days for BS and BS + IN, and at $t = 193$ days for NA.

The inoculum addition to one mesocosm did not improve the performance so much. Looking at the data for the biostimulated mesocosms, the removal efficiency is similar, either in the whole column or only at the bottom. The lower efficiency at the bottom (soil depth = 0.2 m) shows the need to feed oxygen and micronutrients properly in the soil column. The results are fully in line with the results achieved for the microbial activity and reported in Figure 5, where the fluoresceine production is higher for the whole column than for the bottom.

3.4. Viscosity

The application of Equations (2) and (4) shows that the diesel oil viscosity is more influenced by the temperature than the water one.

By Equation (6), the dynamic viscosity of the diesel oil-water mixture was calculated at the starting and the end of the tests. Table 3 shows the data.

Table 3. Dynamic viscosity of diesel oil-water mixture in the tested mesocosms.

Mesocosm	Time (Day)	Diesel Oil Concentration ($\text{kg}_{\text{oil}} \cdot \text{kg}_{\text{soil}}^{-1}$)	Water Content ($\text{kg}_{\text{water}} \cdot \text{kg}_{\text{soil}}^{-1}$)	Volumetric Water Content ($V_{\text{water}} \cdot (V_{\text{oil}} + V_{\text{water}})^{-1}$)	T ($^{\circ}\text{C}$)	Dynamic Viscosity ($\text{mPa} \cdot \text{s}$)
All	0	0.050	0.10	0.625	27	1.3
NA	193	0.049	0.10	0.630	12	2.7
BS	228	0.017	0.10	0.810	12	2.0
BS + IN	228	0.014	0.10	0.838	12	1.9

At the beginning of the test, all the mesocosms had the same water and diesel oil concentration, to say the dynamic viscosity of the mixture had the same value.

At the end of the test, the diesel oil concentration was different in the three mesocosms, as evidenced by the analysis of the soil samples. Therefore, the calculated dynamic viscosity was different, too.

4. Discussion

4.1. Electrical Conductivity

The electrical conductivity (EC) of soil is greatly influenced by the saturation and the salinity of the pore fluid, according, for example, to Archie's law [25].

In the NA mesocosm, hydrated with tap water, the electrical conductivity was quite constant, except for a slight decrease in the first month. In the other two mesocosms, the mineral salt solution added to promote the growth of microorganisms led to having higher initial electrical conductivity, $0.047 \text{ S}\cdot\text{m}^{-1}$. However, EC decreased over time, with a faster rate in BS + IN, in which the EC fell from $0.047 \text{ S}\cdot\text{m}^{-1}$ to $0.007 \text{ S}\cdot\text{m}^{-1}$ in just 15 days, rapidly reaching the value of the NA system, and then maintaining that value without any further variation. In the BS mesocosm, instead, the EC decreased more slowly than in BS + IN: quite rapidly in the first month, and slowly in the other months, until it approached an asymptotic value of about $0.011 \text{ S}\cdot\text{m}^{-1}$.

We assumed that these EC variations were linked to changes in pore fluid salinity, and in this setup, they are probably correlated to a biological process. The only difference between them was that BS + IN had better microorganism adaptation due to the inoculum, and it showed a faster decrease in EC. Past experiments in similar settings showed that inocula of microorganisms adapted to biodegrading a specific contaminant could speed up the degradation process in the first weeks. On the other hand, non-adapted indigenous microorganisms had a longer lag phase, even if, after a long time, the removal efficiency was similar [26].

The EC reduction could be ascribed to the consumption by microorganisms of the nutrient salts added to enhance their activity. After 15 days, the EC of BS + IN was coincident with that of NA, the latter being the mesocosm without salt addition. Looking at the asymptotic values of electrical conductivity in Figure 3 and reported in Table 2, the nutrient solution of BS + IN was completely depleted, while the one added to BS was only partially depleted.

Previous literature did not show the same marked decrease in electrical conductivity values. Mori et al. [12] detected different fluctuations in pore water EC, depending on saturated or unsaturated conditions. Masy et al. [13] performed an electrical resistivity tomography at a lab scale and found that the electrical conductivity increased over time, in both the pore fluid and the bulk. They speculated it was caused by mineral weathering due to bacterial metabolism. The reason for such different behaviour compared to our results could be found in different initial pore water conductivity: about $1.5 \text{ S}\cdot\text{m}^{-1}$ in our case, and about $0.15 \text{ S}\cdot\text{m}^{-1}$ in the work by Masy et al. [13]. This suggests that caution must be taken when comparing different experimental setups of contaminated soil bioremediation. However, these biological processes show a direct, or indirect, measurable electrical signature.

4.2. Electrical Permittivity

The NA mesocosm showed no evidence of variation in the electrical permittivity: the observed small oscillations were due to the temperature dependence of the water permittivity, changing from a value of 88 at 0°C to 64 at 70°C [27]. In the BS + IN mesocosm, the electrical permittivity decreased quickly in the first month and slightly increased during the following 90 days until a constant value was reached. In the BS mesocosm, it can be observed a similar trend, even if at a more gradual rate. Moreover, anomalous behaviour is detected in the first two weeks, which could be explored in future research.

All mesocosms were sealed in the same way, and the NA trend suggests that no or little water was lost in the process. Therefore, the changes in electrical permittivity are not related to water loss. Besides, simple computations by the CRIM method [28] put in evidence that the diesel removal alone cannot explain the decrease of electrical permittivity (of about 1.5–2 units). The variations of the electrical permittivity probably reflect other changes in the soil matrix.

The comparison of the trend of permittivity with electrical conductivity provides further insights. Both the quantities followed a decreasing trend in both biostimulated mesocosms, but changes happened at different times. This is especially evident for BS + IN, in which EC decreased to the asymptotic value in 15 days, while the electrical permittivity reached the lowest value in about one month. This suggests that, if EC is directly related to salinity changes in the pore water due to microbial metabolism, the electrical permittivity changes are not, and they are related to a secondary phenomenon that has a different timescale.

To explain the electrical permittivity decrease, we assume that a biofilm coating gradually formed on the soil surface, affecting the multiphase soil matrix composition and therefore the electrical permittivity. This is supported by a previous study showing that biofilm formation induces a decrease in electrical permittivity [29]. This behaviour is explained because the biofilm, mainly composed of water (90–98%), has an electrical permittivity of about 60, lower than that of pure water ($\epsilon = 80$). The other components, to say the complementary part, are organic. Therefore, in terms of monitoring, a decrease in the electrical permittivity is a sign of the reduction of the water content, and this could support the idea of biofilm generation, even if not verified at the moment.

4.3. Diesel Removal Efficiency

In the biostimulated mesocosms, the removal of diesel oil was 66% and 72%, respectively, for the BS mesocosm and the BS + IN one. In the NA mesocosm, there was a limited removal efficiency, in the order of 2%. Even if the two biostimulated mesocosms had a different trend of electromagnetic properties, evidencing different kinetics of bioremediation, both were able to successfully degrade similar percentages of the contaminant. This supports previous theses about the ability of indigenous microorganisms to degrade hydrocarbons such as diesel oil [14]. The inoculum helps to start faster the degradation, but has a limited effect in the long run, as shown by the removal efficiency data and in previous studies [30].

5. Conclusions

We applied a geophysical methodology to study the degradation processes in contaminated soil at the laboratory scale. The electrical conductivity and electrical permittivity were monitored in three different mesocosms with a TDR probe, and measurements of bacterial activity and diesel degradation were performed to validate the correlation.

The current experimental setup allowed detecting variations in electrical permittivity and conductivity over 228 days. The values of electrical permittivity and conductivity decreased over time in the two biostimulated mesocosms, while remaining rather constant in the natural attenuation one. The electrical conductivity variations were linked to the depletion of the nutrient salts, whereas the electrical permittivity variations were supposed to be due to biofilm formation, even if this hypothesis is unconfirmed. Between the two biostimulated mesocosms, the fastest variation rates of the electromagnetic properties were observed in the inoculated mesocosm, which had enhanced microbial activity compared to the other. The initial rise and the subsequent fall of electrical permittivity values observed in the mesocosm BS were not completely explained, and this feature deserves a future more detailed study.

The electromagnetic properties of soil are influenced by the physical-chemical changes during biodegradation processes. We state that time-domain reflectometry can be a practical and successful indirect method for preliminary screening of the biological activity in

contaminated soil. To formulate quantitative and robust relationships between geophysical response and biological behaviour, further experiments will be required. In this sense, we expect that every empirical relation will be greatly site-dependent since many different factors influence the biodegradation processes in soil.

Future research or preliminary screening of contaminated sites could take advantage of the simple experimental setup proposed in this study, which was demonstrated to be reliable and promising for in-field monitoring of the biological degradation of organic contaminants. It successfully discriminated the different geophysical signatures of different operative conditions in terms of biostimulation (NA vs. BS) and also in terms of bioaugmentation (BS vs. BS + IN).

Future setups at the lab scale may focus on performing the validation analyses in the first 1–2 months from the contamination because it was in the first months that the electromagnetic properties varied most. The method should ensure that the sampling itself does not affect the TDR measurements, for example, by remixing the fluids in the matrix, which tend to distribute not uniformly.

Author Contributions: Conceptualization, A.G. and F.C.; methodology, A.G. and F.C.; software, A.V. and C.M.R.; validation, A.G. and F.C.; data curation, A.V., C.M.R. and F.C.; writing—original draft preparation, A.V., A.G. and F.C.; writing—review and editing, A.V., A.G. and F.C.; supervision, A.G. and F.C. All authors have read and agreed to the published version of the manuscript.

Funding: This research received no external funding.

Institutional Review Board Statement: Not applicable.

Informed Consent Statement: Not applicable.

Data Availability Statement: Not applicable.

Conflicts of Interest: The authors declare no conflict of interest.

References

1. Sarkar, D.; Ferguson, M.; Datta, R.; Birnbaum, S. Bioremediation of petroleum hydrocarbons in contaminated soils: Comparison of biosolids addition, carbon supplementation, and monitored natural attenuation. *Environ. Pollut.* **2005**, *136*, 187–195. [[CrossRef](#)] [[PubMed](#)]
2. Álvarez, M.; Ruberto, L.; Balbo, L.; Cormack, M. Bioremediation of hydrocarbon-contaminated soils in cold regions: Development of a pre-optimized biostimulation biopile-scale field assay in Antarctica. *Sci. Total Environ.* **2017**, *591*, 194–203. [[CrossRef](#)] [[PubMed](#)]
3. Wu, M.; Dick, W.A.; Li, W.; Wang, X.; Yang, Q.; Wang, T.; Xu, L.; Zhang, M.; Chen, L. Bioaugmentation and biostimulation of hydrocarbon degradation and the microbial community in a petroleum-contaminated soil. *Int. Biodeterior. Biodegrad.* **2016**, *107*, 158–164. [[CrossRef](#)]
4. Arato, A.; Wehrer, M.; Birò, B.; Godio, A. Integration of geophysical, geochemical and microbiological data for a comprehensive small-scale characterization of an aged LNAPL-contaminated site. *Environ. Sci. Pollut. Res.* **2014**, *21*, 8948–8963. [[CrossRef](#)] [[PubMed](#)]
5. Zanini, A.; Ghirardi, M.; Emiliani, R. A Multidisciplinary Approach to Evaluate the Effectiveness of Natural Attenuation at a Contaminated Site. *Hydrology* **2021**, *8*, 101. [[CrossRef](#)]
6. Comegna, A.; Coppola, A.; Dragonetti, G.; Sommella, A. Dielectric Response of a Variable Saturated Soil Contaminated by Non-Aqueous Phase Liquids (NAPLs). *Procedia Environ. Sci.* **2013**, *19*, 701–710. [[CrossRef](#)]
7. LaBrecque, D.J.; Ramirez, A.L.; Daily, W.D.; Binley, A.M.; Schima, S.A. ERT monitoring of environmental remediation processes. *Meas. Sci. Technol.* **1996**, *7*, 375–383. [[CrossRef](#)]
8. Davis, C.A.; Pyrak-Nolte, L.J.; Atekwana, E.A.; Werkema, D.D.; Haugen, M.E. Acoustic and electrical property changes due to microbial growth and biofilm formation in porous media. *J. Geophys. Res.* **2010**, *115*, G00G06. [[CrossRef](#)]
9. Atekwana, E.A.; Slater, L.D. Biogeophysics: A new frontier in Earth science research. *Rev. Geophys.* **2009**, *47*, RG4004. [[CrossRef](#)]
10. Cassiani, G.; Binley, A.; Kemna, A.; Wehrer, M.; Flores Orozco, A.; Deiana, R.; Boaga, J.; Rossi, M.; Dietrich, P.; Werban, U.; et al. Noninvasive characterization of the Trecate (Italy) crude-oil contaminated site: Links between contamination and geophysical signals. *Environ. Sci. Pollut. Res.* **2014**, *21*, 8914–8931. [[CrossRef](#)]
11. Revil, A.; Mendonça, C.A.; Atekwana, E.A.; Kullessa, B.; Hubbard, S.S.; Bohlen, K.J. Understanding biogeobatteries: Where geophysics meets microbiology. *J. Geophys. Res.* **2010**, *115*, G00G02. [[CrossRef](#)]
12. Mori, Y.; Suetsugu, A.; Matsumoto, Y.; Fujihara, A.; Suyama, K. Enhancing Bioremediation of Oil-Contaminated Soils by Controlling Nutrient Dispersion Using Dual Characteristics of Soil Pore Structure. *Ecol. Eng.* **2013**, *51*, 237–243. [[CrossRef](#)]

13. Masy, T.; Caterina, D.; Tromme, O.; Lavigne, B.; Thonart, P.; Hiligsmann, S.; Nguyen, F. Electrical Resistivity Tomography to Monitor Enhanced Biodegradation of Hydrocarbons with *Rhodococcus Erythropolis* T902.1 at a Pilot Scale. *J. Contam. Hydrol.* **2016**, *184*, 1–13. [[CrossRef](#)]
14. Raffa, C.M.; Chiampo, F.; Godio, A.; Vergnano, A.; Bosco, F.; Ruffino, B. Kinetics and optimization by response surface methodology of aerobic bioremediation. Geoelectrical parameter monitoring. *Appl. Sci.* **2020**, *10*, 405. [[CrossRef](#)]
15. Vergnano, A.; Godio, A.; Raffa, C.M.; Chiampo, F.; Bosco, F.; Ruffino, B. Time-Domain Reflectometry (TDR) Monitoring at a Lab Scale of Aerobic Biological Processes in a Soil Contaminated by Diesel Oil. *Appl. Sci.* **2019**, *9*, 5487. [[CrossRef](#)]
16. Vergnano, A.; Godio, A.; Raffa, C.M.; Chiampo, F.; Tobon Vasquez, J.A.; Vipiana, F. Open-Ended Coaxial Probe Measurements of Complex Dielectric Permittivity in Diesel-Contaminated Soil during Bioremediation. *Sensors* **2020**, *20*, 6677. [[CrossRef](#)] [[PubMed](#)]
17. UNI EN 932-1:1998; Metodi Di Prova per Determinare Le Proprietà Generali Degli Aggregati. Metodi Di Campionamento. Ente nazionale italiano di unificazione: Milano, Italy, 1998.
18. Schnurer, J.; Rosswall, T. Fluorescein Diacetate Hydrolysis as a Measure of Total Microbial Activity in Soil and Litter. *Appl. Environ. Microbiol.* **1982**, *43*, 1256–1261. [[CrossRef](#)]
19. Adam, G.; Duncan, H. Development of a sensitive and rapid method for the measurement of total microbial activity using fluorescein diacetate (FDA) in a range of soils. *Soil Biol. Biochem.* **2001**, *33*, 943–951. [[CrossRef](#)]
20. Environmental Protection Agency. *Method 3546 "Microwave Extraction"*; Environmental Protection Agency: Georgetown, Guyana, 2007.
21. Environmental Protection Agency. *Method 8015 "Nonhalogenated Organics Using GC/FID"*; Environmental Protection Agency: Georgetown, Guyana, 2003.
22. Perry, R.H.; Green, D.W. (Eds.) *Perry's Chemical Engineers' Handbook*, 8th ed.; McGraw-Hill: New York, NY, USA, 2007; ISBN 978-0-07-142294-9.
23. Nita, I.; Geacai, S. Study of Density and Viscosity Variation with Temperature for Fuels Used for Diesel Engine. *Ovidius Univ. Ann. Chem.* **2011**, *22*, 57–61.
24. Wen, J.; Zhang, J.; Wei, M. Effective Viscosity Prediction of Crude Oil-Water Mixtures with High Water Fraction. *J. Pet. Sci. Eng.* **2016**, *147*, 760–770. [[CrossRef](#)]
25. Archie, G.E. The Electrical Resistivity Log as an Aid in Determining Some Reservoir Characteristics. *Trans. AIME* **1942**, *146*, 54–62. [[CrossRef](#)]
26. Horel, A.; Schiewer, S. Influence of Inocula with Prior Hydrocarbon Exposure on Biodegradation Rates of Diesel, Synthetic Diesel, and Fish-Biodiesel in Soil. *Chemosphere* **2014**, *109*, 150–156. [[CrossRef](#)]
27. Hill, N.E. The Temperature Dependence of the Dielectric Properties of Water. *J. Phys. C Solid State Phys.* **1970**, *3*, 238–239. [[CrossRef](#)]
28. Wharton, R.P.; Hazen, G.A.; Rau, R.N.; Best, D.L. Electromagnetic propagation logging: Advances in technique and interpretation. In Proceedings of the 55th Annual Fall Technical Conference and Exhibition of the SPE of AIME, Dallas, TX, USA, 21–24 September 1980. [[CrossRef](#)]
29. Hoog, N.A.; Mayer, M.J.J.; Miedema, H.; Olthuis, W.; Tomaszewska, A.A.; Paulitsch-Fuchs, A.H.; van den Berg, A. Online Monitoring of Biofouling Using Coaxial Stub Resonator Technique. *Sens. Bio-Sens. Res.* **2015**, *3*, 79–91. [[CrossRef](#)]
30. Horel, A.; Mortazavi, B.; Sobecky, P.A. Input of organic matter enhances degradation of weathered diesel fuel in sub-tropical sediments. *Sci. Total Environ.* **2015**, *533*, 82–90. [[CrossRef](#)] [[PubMed](#)]